

Coupled Oscillators and Dielectric Function

T. Das,¹ C. A. Ullrich,² and U. D. Jentschura¹

¹*Department of Physics and LAMOR, Missouri University of Science and Technology, Rolla, Missouri 65409, USA*

²*Department of Physics and Astronomy, University of Missouri, Columbia, Missouri 65211, USA*

A generalized Sellmeier model, also referred to as the Lorentz–Dirac model, has been used for the description of the dielectric function of a number of technologically important materials in the literature. This model represents the frequency-dependent dielectric function as a sum over Green functions of classical damped harmonic oscillators, much in analogy with the functional form used for the dynamic polarizability of an atom, but with one important addition, namely, a complex-valued oscillator strength in the numerator. Here, we show that this generalized functional form can be justified based on the response function of *coupled* damped oscillators. The encountered analogies suggest an explanation for the generally observed success of the Lorentz–Dirac model in describing the dielectric function of crystals of consummate technological significance.

I. INTRODUCTION

There is no generally accepted universal functional form for the frequency-dependent dielectric function $\epsilon(\omega)$ of a solid. In order to illustrate this statement, we observe that, for the various materials considered in the seminal Ref. [1], vastly different functional forms have been employed in the opening paragraphs which precede the data listings contained in Ref. [1]. Recently, very complicated and involved functional forms have been explored in Ref. [2], for calcium fluoride.

In order to obtain a more consistent picture, it is useful to observe that the dielectric function is (by definition) proportional to the dielectric displacement inside the material. Hence, the quantity $[\epsilon(\omega) - 1]$ must be proportional to the induced polarization P (which equals the volume density of induced dipole moments, see Ref. [3]). In some cases (not solids), the functional form of the dielectric function is known much better. One example is a dilute gas, where [see Eq. (6.132) of Ref. [4]]

$$\begin{aligned}\epsilon(\omega) &= 1 + \frac{N_V}{\epsilon_0} \alpha(\omega) \\ &= 1 + \frac{N_V}{\epsilon_0} \sum_n \frac{f_{n0}}{\hbar^2} \frac{1}{\omega_n^2 - \omega^2 - i\gamma_n \omega}.\end{aligned}\quad (1)$$

Here, $\alpha(\omega)$ is the dipole polarizability of the gas atoms, N_V is their number density, and ϵ_0 is the vacuum permittivity (\hbar is Planck’s unit of action). The resonance frequencies of the atomic transitions are denoted as ω_n , and their respective widths are γ_n (for absolute clarity, we should note that we shall use the term frequency as a synonym for the angular frequency throughout the article, for brevity of notation). The oscillator strengths are denoted as f_{n0} . One notes that the sum over n , a priori, includes all dipole-allowed transitions of the atom.

We have recently used a form analogous to Eq. (1) for the description of the temperature-dependent dielectric function of intrinsic silicon [5],

$$\epsilon(T_\Delta, \omega) = 1 + \sum_{k=1}^{k_{\max}} \frac{a_k(\omega_k^2 - i\gamma'_k \omega)}{\omega_k^2 - \omega^2 - i\omega\gamma_k}, \quad (2)$$

where the oscillator strengths f_{n0} of Eq. (1) are generalized to complex quantities. For intrinsic silicon [5], we were able to achieve a description of the available data with two resonances ($k_{\max} = 2$). In Appendix A.2 of Ref. [5], we argued that the presence of the parameter γ'_k in the numerator of Eq. (2) can be explained on the basis of radiative reaction (Lorentz–Dirac equation). One finds [5, 6] that the temperature-dependence of the parameters a_k (amplitude), ω_k (resonance frequency), γ_k (width) and γ'_k (radiative-reaction width) is smooth and can be described by quadratic polynomials in the variable $T_\Delta = (T - T_0)/T_0$, where T_0 is room temperature (293 K). This functional form is much simpler than, *e.g.*, the ones employed in Ref. [2].

The model given in Eq. (2) was used in Eq. (1) of Ref. [7] for a description of the dielectric function of rutile, in Eq. (4) of Ref. [8] for cubic thallium, and in Eq. (1) of Ref. [9] for sodium nitrate. Furthermore, it was used in Ref. [10] for α -quartz. On the basis of the Lorentz–Dirac equation, the parameter γ'_k should be a positive quantity, as explained in Appendix A.2 of Ref. [5]. This observation raises the question why, for α -quartz [10], one finds negative γ'_k parameters from a fit of the dielectric function. Here, we shall go a different route and explore if one can find an analogy for the functional form (2) considering coupled damped harmonic oscillators.

The motivation for this endeavor stems from the fact that the denominator in Eq. (2), $\omega_k^2 - \omega^2 - i\omega\gamma_k$, is characteristic of a damped harmonic oscillator with resonance frequency ω_k and damping constant γ_k (see Sec. 2.2 of Ref. [4]). One might thus ask to which extent the coupling of oscillators can be related to the complex oscillator strength [manifestly complex numerator $a_k(\omega_k^2 - i\gamma'_k \omega)$] in Eq. (2). Our study thus goes beyond the textbook derivation of the optical susceptibility based on uncoupled classical oscillators [3].

The paper is organized as follows. In Sec. II, we consider two coupled damped oscillators, and we generalize the considerations to three coupled oscillators in Sec. III. The additional role of radiative reaction is discussed in Sec. IV. In Sec. V, we discuss the back-reaction of the dielectric response mediated by photon and phonon fields

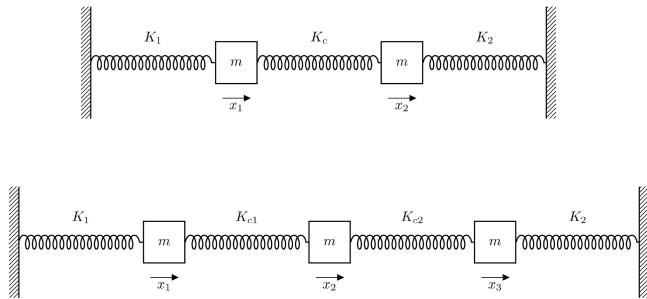


FIG. 1. Schematic view of two and three coupled oscillators (upper and lower panel, respectively).

onto the polarization, and analogies to coupled-oscillator models. Conclusions are reserved for Sec. VI. Atomic units with $\epsilon = 1/(4\pi)$, $\hbar = |e| = 1$, and $c = 1/\alpha$ are employed (see Chap. 2 of Ref. [11]). Here, e is the electron charge and $|e|$ is its modulus, while $\alpha \approx 1/137.036$ is the fine-structure constant. Some technical details are discussed in the Appendix.

II. COUPLED DAMPED OSCILLATORS

A. Derivation of the Signal

In view of the mathematical analogies of damped harmonic oscillators (and their Green functions), analytic expressions for the polarizability of atoms, and the dielectric function of materials (see, *e.g.*, Sec. 6.4.3 of Ref. [4]), it is indicated to consider the signal obtained by driving coupled classical oscillators, and its relation to the mathematical form of the Lorentz–Dirac model given in Eq. (2). We thus consider a system of two coupled oscillators, with coordinates x_1 and x_2 and spring constants K_1 and K_2 for the uncoupled oscillators, and K_c for the coupling (see Fig. 1).

The following two questions will be investigated: (i) Can the response of coupled damped oscillators be described to good numerical accuracy by a functional form of the Lorentz–Dirac model (2), that is, can the signal of coupled damped oscillators alternatively be described by uncoupled oscillators with a complex-valued oscillator strength? (ii) If the answer to (i) is affirmative, are there cases where the radiative-reaction parameter γ' becomes negative upon fitting the signal from the coupled resonances?

Based on Fig. 1 one easily obtains the following dy-

namic equations:

$$m \frac{d^2 x_1}{dt^2} = -\Gamma_1 \frac{dx_1}{dt} - (K_1 + K_c)x_1 + K_c x_2 + F_1(t), \quad (3)$$

$$m \frac{d^2 x_2}{dt^2} = -\Gamma_2 \frac{dx_2}{dt} - (K_2 + K_c)x_2 + K_c x_1 + F_2(t). \quad (4)$$

Here, m denotes the masses of the driven oscillators, which we assume to be equal [12], and the F_i with $i = 1, 2$ are the force terms. The relation of the spring constants to the (unperturbed) resonance frequencies ω_{10} and ω_{20} is $K_1 = m(\omega_{10})^2 = m k_1$, $K_2 = m(\omega_{20})^2 = m k_2$, and we also define $K_c = m\omega_c^2 = m k_c$, $\Gamma_1 = m\gamma_1$, $\Gamma_2 = m\gamma_2$, $F_1 = m f_1$, and $F_2 = m f_2$. In the scaled variables, one obtains

$$\frac{d^2 x_1}{dt^2} = -\gamma_1 \frac{dx_1}{dt} - (k_1 + k_c)x_1 + k_c x_2 + f_1(t), \quad (5a)$$

$$\frac{d^2 x_2}{dt^2} = -\gamma_2 \frac{dx_2}{dt} - (k_2 + k_c)x_2 + k_c x_1 + f_2(t). \quad (5b)$$

Furthermore, we set $f_1 = a_1 E_1$ and $f_2 = a_2 E_2$, where the E_i describe the electric fields, and the a_i are proportional to the number densities of the oscillators. This amounts to a model of coupled oscillators where the spring constants k_1 and k_2 are equal to the squares of the unperturbed resonance frequencies, $k_1 = (\omega_{10})^2$ and $k_2 = (\omega_{20})^2$. The damping constants are γ_1 and γ_2 , and we assume a spring constant k_c for the coupling between the oscillators.

Various physical parameters such as the charge of the driven system are set equal to unity in the above system of equations, and we emphasize that the coupled classical oscillators can at best only be a *model problem* for the full quantum-mechanical system under consideration. We will discuss this point later in Sec. V.

In frequency space, after Fourier transformation, one has $\mathbb{M}(\omega) \cdot \vec{x}(\omega) = \vec{E}(\omega)$,

$$\mathbb{M} \cdot \begin{pmatrix} x_1(\omega) \\ x_2(\omega) \end{pmatrix} = \mathbb{A} \cdot \begin{pmatrix} E_1(\omega) \\ E_2(\omega) \end{pmatrix}, \quad \mathbb{M} = \begin{pmatrix} \mathbb{M}_{11} & \mathbb{M}_{12} \\ \mathbb{M}_{21} & \mathbb{M}_{22} \end{pmatrix}, \quad \mathbb{A} = \begin{pmatrix} \mathbb{A}_{11} & \mathbb{A}_{12} \\ \mathbb{A}_{21} & \mathbb{A}_{22} \end{pmatrix}. \quad (6)$$

The elements of the matrices are easily obtained,

$$\mathbb{M}_{11} = k_1 + k_c - i\gamma_1 \omega - \omega^2, \quad (7a)$$

$$\mathbb{M}_{12} = -k_c = \mathbb{M}_{21}, \quad (7b)$$

$$\mathbb{M}_{22} = k_2 + k_c - i\gamma_2 \omega - \omega^2, \quad (7c)$$

$$\mathbb{A}_{11} = a_1, \quad \mathbb{A}_{22} = a_2, \quad \mathbb{A}_{12} = \mathbb{A}_{21} = 0. \quad (7d)$$

One then finds the inverse relation

$$\begin{pmatrix} x_1(\omega) \\ x_2(\omega) \end{pmatrix} = \mathbb{X} \cdot \begin{pmatrix} E_1(\omega) \\ E_2(\omega) \end{pmatrix}, \quad (8)$$

where the elements of $\mathbb{X} = \mathbb{M}^{-1} \cdot \mathbb{A}$ are as follows,

$$\mathbb{X}_{11} = \frac{N_1}{\mathcal{D}}, \quad \mathbb{X}_{12} = \frac{a_2 k_c}{\mathcal{D}}, \quad (9a)$$

$$\mathbb{X}_{21} = \frac{a_1 k_c}{\mathcal{D}}, \quad \mathbb{X}_{22} = \frac{N_2}{\mathcal{D}}, \quad (9b)$$

$$N_1 = a_1 (k_2 + k_c - \omega^2 - i\gamma_2 \omega), \quad (9c)$$

$$N_2 = a_2 (k_1 + k_c - \omega^2 - i\gamma_1 \omega). \quad (9d)$$

The denominator $\mathcal{D} = \det(\mathbb{M})$ is given by

$$\mathcal{D} = (k_1 + k_c - \omega^2 - i\gamma_1 \omega)(k_2 + k_c - \omega^2 - i\gamma_2 \omega) - k_c^2. \quad (10)$$

For uncoupled oscillators ($k_c = 0$), one recovers the structure of the Sellmeier model (with damping),

$$\mathbb{X}|_{k_c=0} = \begin{pmatrix} \frac{a_1}{k_1 - \omega^2 - i\gamma_1 \omega} & 0 \\ 0 & \frac{a_2}{k_2 - \omega^2 - i\gamma_2 \omega} \end{pmatrix}. \quad (11)$$

For the response of the entire system, one sums over the polarization densities corresponding to the two oscillators. Provided we assume both oscillators to be driven by the same electric field $E_1(\omega) = E_2(\omega) = E(\omega)$, the electric susceptibility $\chi = 4\pi P/E$ is obtained as a quantity proportional to

$$\begin{aligned} \chi(\omega) &\equiv \text{Tr} \left[\mathbb{X} \cdot \begin{pmatrix} 1 \\ 1 \end{pmatrix} \right] = \mathbb{X}_{11} + \mathbb{X}_{12} + \mathbb{X}_{21} + \mathbb{X}_{22} \\ &= \frac{N_1 + (a_1 + a_2)k_c + N_2}{\mathcal{D}}. \end{aligned} \quad (12)$$

Here, we have denoted the trace of a two-component vector \vec{v} (not a 2×2 matrix) as the sum of its elements $v_1 + v_2$. The deviation of the relative dielectric function $\epsilon(\omega)$ from its vacuum value (unity) is $\epsilon(\omega) - 1 = \chi(\omega)$. In order to analyze the resonance structure of the coupled system, it is useful to observe that

$$\mathcal{D} = (\omega_{c1}^2 - \omega^2)(\omega_{c2}^2 - \omega^2) - iW, \quad (13)$$

where

$$\omega_{c1} = \frac{1}{\sqrt{2}} \sqrt{k_1 + k_2 + 2k_c + \gamma_1 \gamma_2 - \sqrt{L}}, \quad (14a)$$

$$\omega_{c2} = \frac{1}{\sqrt{2}} \sqrt{k_1 + k_2 + 2k_c + \gamma_1 \gamma_2 + \sqrt{L}}, \quad (14b)$$

$$L = (k_1 - k_2)^2 + 4k_c^2 + 2(k_1 + k_2 + 2k_c)\gamma_1 \gamma_2 + (\gamma_1 \gamma_2)^2, \quad (14c)$$

$$W = [k_1 \gamma_2 + k_2 \gamma_1 + (\gamma_1 + \gamma_2)(k_c - \omega^2)] \omega. \quad (14d)$$

Provided that $k_c \ll k_1, k_2, |k_1 - k_2|$ (which implies non-degenerate uncoupled oscillator resonance frequencies), one can Taylor-expand in k_c as follows,

$$\omega_{c1} = \sqrt{k_1} + \frac{k_c}{2\sqrt{k_1}} - \frac{(3k_1 + k_2)k_c^2 + 4k_1^2 \gamma_1 \gamma_2}{8(k_1)^{3/2}(k_2 - k_1)} + \dots, \quad (15a)$$

$$\omega_{c2} = \sqrt{k_2} + \frac{k_c}{2\sqrt{k_2}} + \frac{(3k_2 + k_1)k_c^2 + 4k_2^2 \gamma_1 \gamma_2}{8(k_2)^{3/2}(k_2 - k_1)} + \dots. \quad (15b)$$

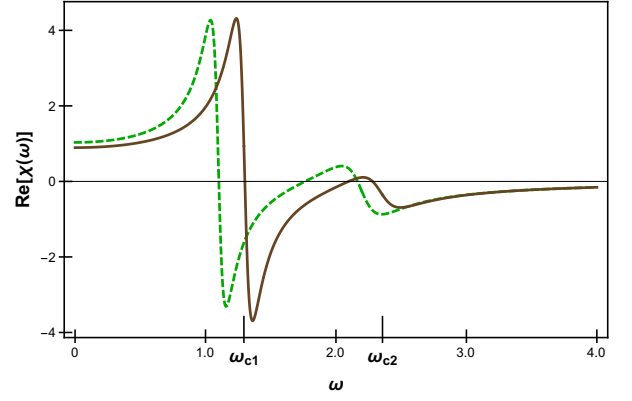


FIG. 2. Real part $\text{Re}[\chi(\omega)]$ of the susceptibility for the model problem given in Eqs. (12), (18) and (20). The resonance frequencies of the coupled system (solid brown curve) are shifted toward higher frequencies in comparison to the resonance frequencies of the uncoupled system (dashed green curve), consistent with Eqs. (14) and (15).

In obtaining these expressions we have assumed that $k_c \sim \gamma_1 \sim \gamma_2$ are small parameters, and we have expanded up to second order in these three parameters. Provided that W is small near the resonances (it is proportional to the width parameters γ_1 and γ_2), we can assume that the shifted resonance frequencies ω_{c1} and ω_{c2} approximate the resonance frequencies of the coupled system reasonably well.

The imaginary part of the signal at the first resonance frequency can be obtained analytically as follows,

$$\text{Im}[\chi(\omega_{c1})] = \frac{a_2 k_1 + a_1 k_2 + (a_1 + a_2)(2k_c - \omega_{c1}^2)}{\omega_{c1} [k_2 \gamma_1 + k_1 \gamma_2 + (\gamma_1 + \gamma_2)(k_c - \omega_{c1}^2)]}. \quad (16)$$

At the second resonance frequency, one finds

$$\text{Im}[\chi(\omega_{c2})] = \frac{a_2 k_1 + a_1 k_2 + (a_1 + a_2)(2k_c - \omega_{c2}^2)}{\omega_{c2} [k_2 \gamma_1 + k_1 \gamma_2 + (\gamma_1 + \gamma_2)(k_c - \omega_{c2}^2)]}. \quad (17)$$

B. Exact Decomposition

To illustrate the behavior of the coupled system we now consider a numerical example with the following parameters:

$$a_1 = a_2 = 1, \quad k_1 = 1.21, \quad k_2 = 4.84, \quad (18a)$$

$$\gamma_1 = 0.12, \quad \gamma_2 = 0.33. \quad (18b)$$

We shall contrast the cases

$$k_c = 0.57 \quad \text{versus} \quad k_c = 0. \quad (18c)$$

Based on Eq. (14), one finds the following coupled resonance frequencies for $k_c = 0.57$,

$$\omega_{c1} = 1.29431, \quad \omega_{c2} = 2.35677, \quad (19)$$

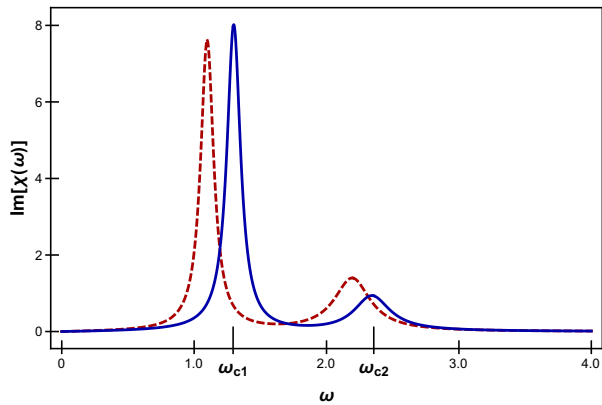


FIG. 3. Same as Fig. 2, but for the imaginary part of the polarization $\text{Im}[\chi(\omega)]$, for the model problem given in Eqs. (18) and (20). The resonance frequencies of the coupled system (solid blue curve) are shifted toward higher frequencies in comparison to the resonance frequencies of the uncoupled system (dashed red curve) [see Eqs. (14) and (15)].

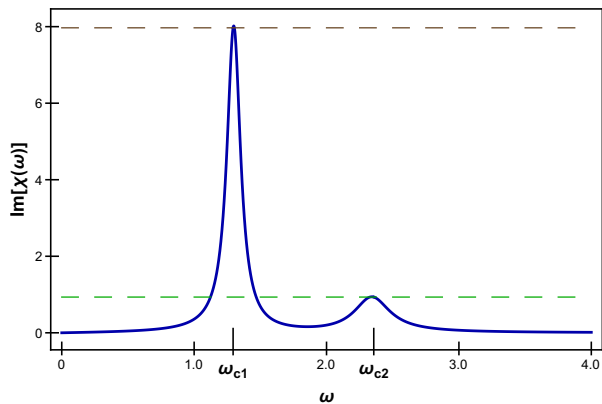


FIG. 4. Imaginary part $\text{Im}[\chi(\omega)]$ for the model problem given in Eqs. (18) and (20), indicating the resonance positions (14) and the precise values of the maxima of the imaginary parts given in Eqs. (16) and (17). The upper dashed line designates $\text{Im}[\chi(\omega_{c1})]$, while the lower dashed line designates $\text{Im}[\chi(\omega_{c2})]$.

while for $k_c = 0$, the frequencies are equal to the uncoupled ones, namely, $\omega_{10} = 1.1$ and $\omega_{20} = 2.2$. In Figs. 2 and 3, we plot the real and imaginary parts of the susceptibility $\chi(\omega)$ defined in Eq. (12), which is related to the dielectric function,

$$\epsilon(\omega) = 1 + \chi(\omega). \quad (20)$$

As evident from Figs. 2 and 3, both resonance frequencies of the coupled system are higher than the corresponding one of the uncoupled system. This is consistent with Eq. (15). The imaginary parts of $\chi(\omega)$ at the resonances [see Eqs. (16) and (17)] are explicitly indicated in Fig. 4.

We now report on a surprising observation: On the basis of a relatively involved partial-fraction decomposition (see Appendix A), one finds that $\chi(\omega)$ can be

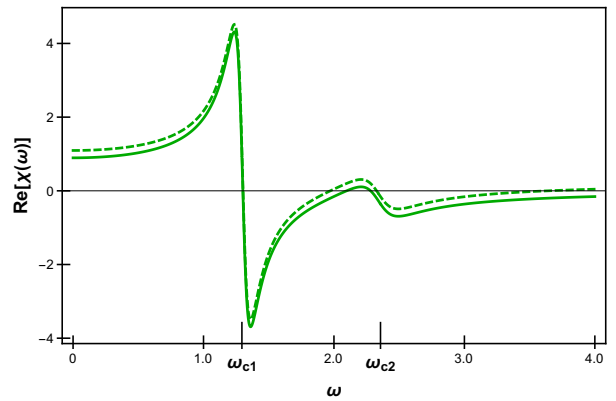


FIG. 5. Illustration of the exact equality of the real part $\text{Re}[\chi(\omega)]$ defined in Eq. (12) (solid curve) and the Lorentz–Dirac (generalized Sellmeier) representation given in Eq. (21) (dashed line), for the parameters given in Eqs. (18) and (22). The Lorentz–Dirac representation has the analytic structure of Eq. (2). An offset of +0.2 is applied to the representation (21) in order to make the two curves visually discernible.

identically expressed as follows,

$$\chi(\omega) = \frac{\tilde{a}_1 [(\tilde{\omega}_1)^2 - i\tilde{\gamma}'_1\omega]}{(\tilde{\omega}_1)^2 - \omega^2 - i\tilde{\gamma}_1\omega} + \frac{\tilde{a}_2 [(\tilde{\omega}_2)^2 - i\tilde{\gamma}'_2\omega]}{(\tilde{\omega}_2)^2 - \omega^2 - i\tilde{\gamma}_2\omega}, \quad (21)$$

with the parameters

$$\tilde{a}_1 = 0.767\,032\,409\,078, \quad \tilde{\omega}_1 = 1.301\,169\,279\,269, \quad (22a)$$

$$\tilde{\gamma}'_1 = -2.064\,444\,521\,508 \times 10^{-2}, \quad (22b)$$

$$\tilde{\gamma}_1 = 0.124\,833\,194\,922, \quad (22c)$$

$$\tilde{a}_2 = 0.128\,194\,836\,781, \quad \tilde{\omega}_2 = 2.344\,347\,861\,458, \quad (22d)$$

$$\tilde{\gamma}'_2 = 0.123\,522\,592\,212, \quad \tilde{\gamma}_2 = 0.325\,166\,805\,078. \quad (22e)$$

The result (21) precisely has the structure of Eq. (2) and provides for an exact decomposition of the response of the coupled oscillators in terms of resonators with complex oscillator strengths. The fact that the susceptibility $\chi(\omega)$ of the coupled oscillators can be expressed in the form (21) becomes understandable if one observes that the denominator \mathcal{D} defined in Eq. (10) is a fourth-degree polynomial in ω and thus has four roots in the complex plane, with negative imaginary parts for the roots $\pm\sqrt{(\tilde{\omega}_1)^2 - (\tilde{\gamma}_1)^2/4} - i\tilde{\gamma}_1/2$ and $\pm\sqrt{(\tilde{\omega}_2)^2 - (\tilde{\gamma}_2)^2/4} - i\tilde{\gamma}_2/2$. One notes that numerically, $\tilde{\omega}_1 \approx \omega_{c1}$ and $\tilde{\omega}_2 \approx \omega_{c2}$, but there is no equality (see also Appendix A). The fact that $\tilde{\gamma}'_1$ is negative confirms that coupled oscillators may introduce what would be referred to as a negative radiation-reaction term in the sense of the considerations of Appendix A.2 of Ref. [5]. The representation (21) precisely has the structure of Eq. (2). In Fig. 5, the equality of the expressions in Eq. (12) and in (21) is represented visually.

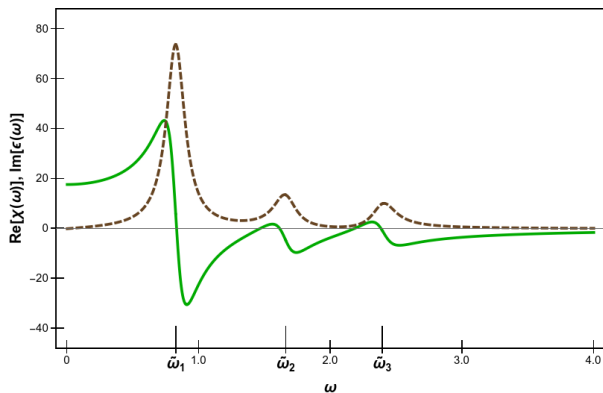


FIG. 6. Real and imaginary parts of $\chi(\omega)$ from Eq. (30) for three coupled oscillators, with parameters given in Eqs. (29) and (31). The solid curve shows the real part $\text{Re}[\chi(\omega)]$, while the dashed curve depicts the imaginary part $\text{Im}[\chi(\omega)]$.

III. THREE COUPLED OSCILLATORS

We generalize the considerations of Sec. II to three coupled oscillators, with coordinates x_1 , x_2 , and x_3 (see Fig. 1). The equations of motion are obtained as follows,

$$\frac{d^2 x_1}{dt^2} = -\gamma_1 \frac{dx_1}{dt} - k_1 x_1 + k_{c1} (x_2 - x_1), \quad (23a)$$

$$\frac{d^2 x_2}{dt^2} = -\gamma_2 \frac{dx_2}{dt} + k_{c1} (x_1 - x_2) + k_{c2} (x_3 - x_2), \quad (23b)$$

$$\frac{d^2 x_3}{dt^2} = -\gamma_3 \frac{dx_3}{dt} - k_2 x_3 + k_{c2} (x_2 - x_3). \quad (23c)$$

In frequency space, one has $\mathbb{M}(\omega) \cdot \vec{x}(\omega) = \mathbb{A} \cdot \vec{E}(\omega)$,

$$\mathbb{M} \cdot \begin{pmatrix} x_1(\omega) \\ x_2(\omega) \\ x_3(\omega) \end{pmatrix} = \mathbb{A} \cdot \begin{pmatrix} E_1(\omega) \\ E_2(\omega) \\ E_3(\omega) \end{pmatrix}, \quad (24)$$

$$\mathbb{M} = \begin{pmatrix} \mathbb{M}_{11} & \mathbb{M}_{12} & \mathbb{M}_{13} \\ \mathbb{M}_{21} & \mathbb{M}_{22} & \mathbb{M}_{23} \\ \mathbb{M}_{31} & \mathbb{M}_{32} & \mathbb{M}_{33} \end{pmatrix}. \quad (25)$$

The \mathbb{A} matrix is obtained as follows,

$$\mathbb{A} = \text{diag}(a_1, a_2, a_3). \quad (26)$$

The nonvanishing elements of the \mathbb{M} matrix are easily obtained,

$$\mathbb{M}_{11} = k_1 + k_{c1} - i\gamma_1 \omega - \omega^2, \quad (27a)$$

$$\mathbb{M}_{12} = -k_{c1} = \mathbb{M}_{21}, \quad (27b)$$

$$\mathbb{M}_{22} = k_{c1} + k_{c2} - i\gamma_2 \omega - \omega^2, \quad (27c)$$

$$\mathbb{M}_{23} = -k_{c2} = \mathbb{M}_{32}, \quad (27d)$$

$$\mathbb{M}_{33} = k_2 + k_{c2} - i\gamma_3 \omega - \omega^2, \quad (27e)$$

while $\mathbb{M}_{13} = \mathbb{M}_{31} = 0$. Let us define $\mathbb{X} = \mathbb{M}^{-1} \cdot \mathbb{A}$. In analogy to Eq. (12), we obtain, for $E_1(\omega) = E_2(\omega) = E_3(\omega) = E(\omega)$, the susceptibility as

$$\chi(\omega) \equiv \text{Tr} \left[\mathbb{X} \cdot \begin{pmatrix} 1 \\ 1 \\ 1 \end{pmatrix} \right] = \sum_{i,j=1}^3 \mathbb{X}_{ij} = \frac{Q(\omega)}{\det(\mathbb{M})}, \quad (28)$$

where $\det(\mathbb{M})$ is the determinant of the \mathbb{M} matrix and $Q(\omega)$ constitutes a sixth-degree polynomial in ω , which is not explicitly given here. Analytic formulas analogous to those presented in Appendix A are harder to obtain than for the case of two coupled oscillators, in view of the fact that the determinant $\det(\mathbb{M})$, for three as opposed to two coupled oscillators, constitutes a sixth-degree polynomial in ω , for which there are in general no known analytic solutions.

We thus consider the numerical example

$$k_1 = 0.5, \quad k_{c1} = 1.3, \quad k_{c2} = 1.8, \quad k_2 = 2.5, \quad (29a)$$

$$a_1 = 1.5, \quad a_2 = 0.5, \quad a_3 = 3.0, \quad (29b)$$

$$\gamma_1 = 0.2, \quad \gamma_2 = 0.1, \quad \gamma_3 = 0.3. \quad (29c)$$

Via a partial-fraction decomposition analogous to the one outlined in Appendix A (but more complicated because of the more complex nature of the entire expression encountered for three oscillators), one arrives at the result

$$\chi(\omega) = \sum_{k=1}^3 \frac{\tilde{a}_k [(\tilde{\omega}_k)^2 - i\tilde{\gamma}'_k \omega]}{(\tilde{\omega}_k)^2 - \omega^2 - i\tilde{\gamma}_k \omega}, \quad (30)$$

with the parameters

$$\tilde{a}_1 = 15.139\,958\,453, \quad \tilde{\omega}_1 = 0.828\,692\,566, \quad (31a)$$

$$\tilde{\gamma}'_1 = -1.337\,923\,149 \times 10^{-2}, \quad (31b)$$

$$\tilde{\gamma}_1 = 1.713\,373\,478 \times 10^{-2}, \quad (31c)$$

$$\tilde{a}_2 = 1.642\,138\,137, \quad \tilde{\omega}_2 = 1.662\,516\,990, \quad (31d)$$

$$\tilde{\gamma}'_2 = -2.297\,066\,450 \times 10^{-2}, \quad (31e)$$

$$\tilde{\gamma}_2 = 2.089\,767\,725 \times 10^{-1}, \quad (31f)$$

$$\tilde{a}_3 = 0.919\,509\,649, \quad \tilde{\omega}_3 = 2.395\,819\,425, \quad (31g)$$

$$\tilde{\gamma}'_3 = 6.305\,219\,871 \times 10^{-1}, \quad (31h)$$

$$\tilde{\gamma}_3 = 2.196\,858\,795 \times 10^{-1}. \quad (31i)$$

Again, two of the γ' parameters are negative ($\tilde{\gamma}'_1$ and $\tilde{\gamma}'_2$), and thus, the possibility of explaining the presence of negative γ' due to the coupling of resonances is confirmed (see Ref. [10] for an application to α -quartz). The spectrum (30), for the parameters given in Eq. (29), is shown in Fig. 6.

IV. COUPLED DAMPED OSCILLATORS WITH RADIATIVE REACTION

At this point, both questions raised near the beginning of Sec. II have been answered affirmatively. There is

one more point to address. Namely, in the course of the investigations [5], a situation was encountered where the first resonance of the Lorentz–Dirac type, in a model of the form (2) with $k_{\max} = 2$, when taken alone, would induce a small negative imaginary part in $\epsilon(\omega)$ for small ω , while the sum over both resonances does not suffer from this problem.

A third question thus emerges: (iii) Is it possible to find a model system of two coupled oscillators, with radiative reaction, which generates a negative imaginary part from the first of two resonances, while the imaginary part for the sum of both resonances remains positive?

Let us first observe that, with the inclusion of radiative reaction, the system (5) of equations is modified to read

$$\frac{d^2 x_1}{dt^2} = -\gamma_1 \frac{dx_1}{dt} - (k_1 + k_c) x_1 + k_c x_2 + \mathcal{F}_1(t), \quad (32)$$

$$\frac{d^2 x_2}{dt^2} = -\gamma_2 \frac{dx_2}{dt} - (k_2 + k_c) x_2 + k_c x_1 + \mathcal{F}_2(t). \quad (33)$$

In frequency space this is equivalent to the matrix equation $\mathbb{M} \cdot \vec{x}(\omega) = \vec{\mathcal{F}}(\omega)$, where the elements of the \mathbb{M} matrix are given in Eq. (7). Here, \mathcal{F} is a generalized force, which includes radiative reaction (for which there is no classical analogue). With radiation-reaction included, $\vec{\mathcal{F}}(\omega)$ takes the form

$$\begin{pmatrix} \mathcal{F}_1 \\ \mathcal{F}_2 \end{pmatrix} = \begin{pmatrix} R_{11} & R_{12} \\ R_{21} & R_{22} \end{pmatrix} \cdot \begin{pmatrix} E_1 \\ E_2 \end{pmatrix}, \quad (34)$$

where

$$R_{11} = a_1(k_1 - i\gamma'_1\omega), \quad (35a)$$

$$R_{12} = 0 = R_{21}, \quad (35b)$$

$$R_{22} = a_2(k_2 - i\gamma'_2\omega). \quad (35c)$$

We reemphasize that there is no classical analogue for radiative reaction. One thus has the relation

$$\begin{pmatrix} x_1(\omega) \\ x_2(\omega) \end{pmatrix} = \mathbb{X} \cdot \begin{pmatrix} E_1(\omega) \\ E_2(\omega) \end{pmatrix}, \quad (36)$$

where E_1 and E_2 are the electric fields driving the two oscillators. The elements of $\mathbb{X} = \mathbb{M}^{-1} \cdot \mathbb{R}$ are as follows,

$$\mathbb{X}_{11} = \frac{\mathcal{N}_1}{\mathcal{D}}, \quad \mathbb{X}_{12} = \frac{a_2 k_c (k_2 - i\gamma'_2\omega)}{\mathcal{D}}, \quad (37a)$$

$$\mathbb{X}_{22} = \frac{a_1 k_c (k_1 - i\gamma'_1\omega)}{\mathcal{D}}, \quad \mathbb{X}_{21} = \frac{\mathcal{N}_2}{\mathcal{D}}, \quad (37b)$$

where

$$\mathcal{N}_1 = a_1(k_1 - i\gamma'_1\omega)(k_2 + k_c - \omega^2 - i\gamma_2\omega), \quad (37c)$$

$$\mathcal{N}_2 = a_2(k_2 - i\gamma'_2\omega)(k_1 + k_c - \omega^2 - i\gamma_1\omega). \quad (37d)$$

The denominator in Eqs. (37a) and (37b) has the structure $\mathcal{D} = \det(\mathbb{M})$, where \mathbb{M} is given in Eq. (7).

We consider the following example parameters:

$$a_1 = a_2 = 1, \quad k_c = 0.4, \quad k_1 = 1.2, \quad (38a)$$

$$k_2 = 2.4, \quad \gamma_1 = 0.12, \quad \gamma_2 = 0.2, \quad (38b)$$

$$\gamma'_1 = 0.2, \quad \gamma'_2 = 0.05, \quad (38c)$$

and the susceptibility is given by

$$\chi(\omega) = \mathbb{X}_{11} + \mathbb{X}_{12} + \mathbb{X}_{21} + \mathbb{X}_{22}, \quad (39)$$

in full analogy with Eq. (12). One finds the following, *exact* decomposition,

$$\chi(\omega) = \frac{\tilde{a}_1 [(\tilde{\omega}_1)^2 - i\tilde{\gamma}'_1\omega]}{(\tilde{\omega}_1)^2 - \omega^2 - i\tilde{\gamma}_1\omega} + \frac{\tilde{a}_2 [(\tilde{\omega}_2)^2 - i\tilde{\gamma}'_2\omega]}{(\tilde{\omega}_2)^2 - \omega^2 - i\tilde{\gamma}_2\omega}, \quad (40)$$

with the parameters

$$\tilde{a}_1 = 1.55425744 \quad \tilde{\omega}_1 = 1.216304356, \quad (41a)$$

$$\tilde{\gamma}'_1 = 0.128975503, \quad \tilde{\gamma}_1 = 0.126738002, \quad (41b)$$

$$\tilde{a}_2 = 0.445742559, \quad \tilde{\omega}_2 = 1.708832956, \quad (41c)$$

$$\tilde{\gamma}'_2 = 0.111137838, \quad \tilde{\gamma}_2 = 0.193261997. \quad (41d)$$

In view of the inequality $\tilde{\gamma}'_1 > \tilde{\gamma}_1$, the first resonance term creates a small negative imaginary part for small ω . Numerically, one verifies that

$$\left. \frac{\partial}{\partial \omega} \frac{\tilde{a}_1 [(\tilde{\omega}_1)^2 - i\tilde{\gamma}'_1\omega]}{(\tilde{\omega}_1)^2 - \omega^2 - i\tilde{\gamma}_1\omega} \right|_{\omega=0} = -i 2.3507 \times 10^{-3}. \quad (42)$$

By contrast, with χ given in Eq. (40), one has the following numerical result for the derivative at ω , for the full susceptibility χ ,

$$\left. \frac{\partial}{\partial \omega} \chi(\omega) \right|_{\omega=0} = +i 1.0185 \times 10^{-2}. \quad (43)$$

Because $\text{Im}[\chi(\omega = 0)] = 0$, the derivative at $\omega = 0$ indicates the presence or absence of a negative imaginary part for small driving frequency ω . One concludes that it is easily possible to devise a model problem of two coupled oscillators (which includes radiative damping), where one term in the decomposition (41) generates a spurious negative imaginary part (42) of the dielectric function $\epsilon = 1 + \chi$ for small ω , while the full susceptibility χ has a positive imaginary part [see Eq. (43)], in accordance with the causality principle, and, from a different point of view, the second law of thermodynamics.

V. BACK-REACTION AND COUPLING

It is very well known that, if one considers the response of dense materials to incident electromagnetic radiation, the back-reaction of the emitted radiation onto the constituents of the solid needs to be considered. On the classical level this is manifest in the derivation of the Clausius–Mossotti equation (see, *e.g.*, Refs. [13, 14] or Sec. 6.4.4 of Ref. [4]). Namely, in order to derive the Clausius–Mossotti equation, one considers an external electric field which orients the dipoles inside the solid. However, the oriented dipoles, in turn, generate an additional electric field which needs to be added to the ambient external electric field which led to the orientation of the dipoles in the first place. Relating the polarization

generated with the local electric field, which takes the field generated by all other polarized dipoles in the solid into account, one obtains the Clausius–Mossotti equation [4, 13, 14]. For a dense material, it is insufficient to consider individual, isolated excitations like in a dilute gas.

Now, it is well known that the oscillators in a solid are coupled via the crystal lattice. For low-energy resonances, this is clear because the phonons themselves are quantized lattice vibrations [13]. In Ref. [15], a Hamiltonian has been explored which describes the coupling of the electrons in the crystal lattice to the (quantized) phonon field. The structure of the phonon and electron-phonon coupling terms is reminiscent of coupled harmonic oscillators.

For higher-energy resonances (with an energy higher than vibrational excitations, *e.g.*, optical resonances), one needs to consider the back-reaction of the substantial polarization field (namely, the additional electric field due to all the polarized dipoles inside the crystal) onto a specific reference atom, locally within the lattice (this back-reaction effect is incorporated into the Clausius–Mossotti equation on the classical level). In the optical regime, the back-reaction is primarily of electromagnetic origin. In Ref. [16], this back-reaction mechanism is explored on the level of quantized fields: The Hamiltonian considered in Ref. [16] contains a photon term with a dipole coupling to the Kohn–Sham orbitals obtained from density-functional theory [17, 18], via the total dipole moment $\vec{R}(t)$ defined in the text following Eq. (6) of Ref. [16]. In turn, the photon field enters the mean-field exchange-correlation potential [see Eqs. (5) and (6) of Ref. [16]]. The end result is that in Ref. [16], the authors obtain quantized self-consistent field equations, which take the back-reaction of matter onto the photon field into account (and vice versa). In the text following Eq. (8) of Ref. [16], explicit reference is made to an analogy of the obtained self-consistent equations to coupled harmonic oscillators.

In both cases considered above (lattice vibrations and optical resonance), the oscillations due to lattice vibrations, and those due to electronic excitations of the atoms in the crystal lattice, are coupled. These observations suggest that, in order to generalize the treatment sketched here for classical oscillators to the fully quantized formalism, the analogies of the quantized systems to coupled oscillators pointed out in Refs. [15, 16] should be very useful.

VI. CONCLUSIONS

In this paper, we have raised three questions (see Sec. II and IV) about the suitability of the Lorentz–Dirac model (2), which could be answered affirmatively in view of the analogies of quantum resonances in solids with coupled oscillators discussed in Sec. V.

Let us recall the first question, slightly paraphrased:

(i) Can the response of coupled damped oscillators be described to good numerical accuracy by a functional form of the Lorentz–Dirac model (2), that is, can the signal of coupled damped oscillators alternatively be described by uncoupled oscillators with a complex-valued oscillator strength? The answer is affirmative: in the case of two coupled oscillators [Eq. (21)], three coupled oscillators [Eq. (30)], and two coupled oscillators with radiative reaction [Eq. (40)], it was possible to bring the model polarization response of the model system (coupled oscillators) into a form which is exactly of the Lorentz–Dirac form (2).

The second question was: (ii) Are there cases where the radiative-reaction parameter γ' becomes negative upon fitting the signal from the coupled resonances? The answer is again affirmative: The γ'_1 parameter in the example cases given in Eq. (21) (for two coupled oscillators) and for γ'_1 and γ'_2 in Eq. (30) (for three coupled oscillators) are negative. These results, obtained for our model problems, are analogous to the presence of negative γ' parameters for α -quartz [10].

The third question was asked in Sec. IV: (iii) Is it possible to find a model system of two coupled oscillators, with radiative reaction, which generates a negative imaginary part from the first of two resonances, while the imaginary part for the sum of both resonances remains positive? Again, the answer is yes: For the parameters given in Eq. (41), the first resonance, upon the inclusion of radiative reaction, gives rise to a negative imaginary part for the model dielectric function [see Eq. (42)], while the full response of the system does not follow this behavior [see Eq. (43)].

Our considerations support the suitability of the functional form (2) for the description of the dielectric function of solids. In this paper, we only considered the explicit cases of two and three oscillators. The functional form (2) is given for an arbitrary number of oscillators. The analytic and numerical results presented here strongly suggest that our findings hold for more than three oscillators; a general analytic proof, however, is beyond the scope of this paper.

We also discussed the significance of our classical coupled oscillator model, in the sense of a possible correspondence to a quantum system (see Sec. V). Our findings suggest that generalized oscillator strengths (not necessarily positive and real) can occur when different subsystems are coupled and can exchange (or dissipate) energy. Analogies to time-dependent density-functional theory (TDDFT), when coupled self-consistently to photons, have been explored in Ref. [16], with corresponding analogies to coupled oscillators. Our findings indicate that the self-consistent inclusion of back-reaction effects could be an essential step in first-principles approaches to optical absorption spectra in the presence of electron-phonon interactions [19–21].

Finally, let us point out an interesting observation: *a priori*, one might assume that the Clausius–Mossotti model studied in Ref. [5] might provide for a better rep-

resentation of the response of intrinsic silicon (certainly, a dense material) than the Lorentz–Dirac model for the dielectric function. However, if we conclude that the back-reaction of the coupled oscillators is already encoded in the complex oscillator strengths, and does not necessitate to additionally invoke the Clausius–Mossotti inspired functional form for the dielectric function studied in Ref. [5], then it becomes immediately understandable why the Lorentz–Dirac and Clausius–Mossotti functional forms were seen to yield equally satisfactory representations of the updated experimental data for the real and imaginary parts of the dielectric function of intrinsic silicon studied in Ref. [5].

As a final remark, we observe that the model based on

the functional form (2) turns out to be physically well motivated and grounded in a coupled oscillator model. The applicability of the model (2) for solids of technological significance (*e.g.*, calcium fluoride) is currently being studied further [22–28].

ACKNOWLEDGMENTS

Stimulating conversations with Professor Vladimir M. Mostepanenko are gratefully acknowledged. T. D. and U. D. J. were supported by NSF grant PHY–2110294. C. A. U. acknowledges support from NSF grant DMR–2149082.

Appendix A: An Important Identity

If we attempt to show that the signal of coupled oscillators, as given in Eq. (12), can be represented in the Lorentz–Dirac functional form, then we should investigate the functional form of the common denominator \mathcal{D} in closer detail [see Eq. (10)]. First, we observe that since \mathcal{D} corresponds to a retarded Green function (of the coupled-oscillator system), the roots of the equation $\mathcal{D} = 0$ have a negative imaginary part. We denote the values of the roots as $\omega = \bar{\omega}_i$ (with $i = 1, 2, 3, 4$), $\bar{\omega}_1 = \mathcal{E}_1 - i\tilde{\gamma}_1/2$, $\bar{\omega}_2 = -\mathcal{E}_1 - i\tilde{\gamma}_1/2$, $\bar{\omega}_3 = \mathcal{E}_2 - i\tilde{\gamma}_2/2$, $\bar{\omega}_4 = -\mathcal{E}_2 - i\tilde{\gamma}_2/2$; all of them have a negative imaginary part. Our initial expression given in Eq. (12) therefore has the structure

$$G = \frac{A + iB\omega + C\omega^2}{(\mathcal{E}_1 - \frac{i}{2}\tilde{\gamma}_1 - \omega)(\mathcal{E}_1 + \frac{i}{2}\tilde{\gamma}_1 + \omega)(\mathcal{E}_2 - \frac{i}{2}\tilde{\gamma}_2 - \omega)(\mathcal{E}_2 + \frac{i}{2}\tilde{\gamma}_2 + \omega)}, \quad (\text{A1})$$

where $A, B, C, \mathcal{E}_1, \mathcal{E}_2, \tilde{\gamma}_1$ and $\tilde{\gamma}_2$ are constants. By a partial-fraction decomposition, one can show that

$$G = H \left(\frac{A_1 + iB_1\omega}{D_1} + \frac{A_2 + iB_2\omega}{D_2} \right). \quad (\text{A2})$$

The parameters can be expressed as

$$H = \frac{1}{[4(\mathcal{E}_1 - \mathcal{E}_2)^2 + (\tilde{\gamma}_1 - \tilde{\gamma}_2)^2][4(\mathcal{E}_1 - \mathcal{E}_2)^2 + (\tilde{\gamma}_1 + \tilde{\gamma}_2)^2]}, \quad (\text{A3a})$$

$$A_1 = 4A[4(\mathcal{E}_2^2 - \mathcal{E}_1^2) + 3\tilde{\gamma}_1^2 - 4\tilde{\gamma}_1\tilde{\gamma}_2 + \tilde{\gamma}_2^2] + 4B(4\mathcal{E}_1^2 + \tilde{\gamma}_1^2)(\tilde{\gamma}_2 - \tilde{\gamma}_1) + C(4\mathcal{E}_1^2 + \tilde{\gamma}_1^2)(4(-\mathcal{E}_1^2 + \mathcal{E}_2^2) - \tilde{\gamma}_1^2 + \tilde{\gamma}_2^2), \quad (\text{A3b})$$

$$A_2 = 4A[4(\mathcal{E}_1^2 - \mathcal{E}_2^2) + \tilde{\gamma}_1^2 - 4\tilde{\gamma}_1\tilde{\gamma}_2 + 3\tilde{\gamma}_2^2] + 4B(4\mathcal{E}_2^2 + \tilde{\gamma}_2^2)(\tilde{\gamma}_1 - \tilde{\gamma}_2) + C(4\mathcal{E}_2^2 + \tilde{\gamma}_2^2)(4(\mathcal{E}_1^2 - \mathcal{E}_2^2) + \tilde{\gamma}_1^2 - \tilde{\gamma}_2^2), \quad (\text{A3c})$$

$$B_1 = 16A(\tilde{\gamma}_2 - \tilde{\gamma}_1) + 4B(4(\mathcal{E}_1^2 - \mathcal{E}_2^2) + \tilde{\gamma}_1^2 - \tilde{\gamma}_2^2) + 4C(4\mathcal{E}_1^2\tilde{\gamma}_2 - 4\mathcal{E}_2^2\tilde{\gamma}_1 + \tilde{\gamma}_1\tilde{\gamma}_2(\tilde{\gamma}_1 - \tilde{\gamma}_2)), \quad (\text{A3d})$$

$$B_2 = 16A(\tilde{\gamma}_1 - \tilde{\gamma}_2) + 4B(4(-\mathcal{E}_1^2 + \mathcal{E}_2^2) - \tilde{\gamma}_1^2 + \tilde{\gamma}_2^2) + 4C(4\mathcal{E}_2^2\tilde{\gamma}_1 - 4\mathcal{E}_1^2\tilde{\gamma}_2 + \tilde{\gamma}_1\tilde{\gamma}_2(\tilde{\gamma}_2 - \tilde{\gamma}_1)), \quad (\text{A3e})$$

$$D_1 = \mathcal{E}_1^2 + \frac{1}{4}\tilde{\gamma}_1^2 - i\tilde{\gamma}_1\omega - \omega^2 = \tilde{\omega}_1^2 - i\tilde{\gamma}_1\omega - \omega^2, \quad \tilde{\omega}_1 = \sqrt{\mathcal{E}_1^2 + \frac{1}{4}\tilde{\gamma}_1^2}, \quad (\text{A3f})$$

$$D_2 = \mathcal{E}_2^2 + \frac{1}{4}\tilde{\gamma}_2^2 - i\tilde{\gamma}_2\omega - \omega^2 = \tilde{\omega}_2^2 - i\tilde{\gamma}_2\omega - \omega^2. \quad \tilde{\omega}_2 = \sqrt{\mathcal{E}_2^2 + \frac{1}{4}\tilde{\gamma}_2^2}. \quad (\text{A3g})$$

An application of the identity (A2) leads to the result (21). One notes that the quantities ω_{c1} and ω_{c2} constitute approximations to $\tilde{\omega}_1$ and $\tilde{\omega}_2$, but there is no equality: Namely, at ω_{c1} and ω_{c2} , the real part of the denominator \mathcal{D} defined in Eq. (10) vanishes. By contrast, the complex roots of the entire (complex rather than real) denominator polynomial (in ω) are denoted as $\bar{\omega}_i$ with $i = 1, 2, 3, 4$.

- [1] E. D. Palik, *Handbook of Optical Constants of Solids* (Academic Press, San Diego, 1985).
- [2] T. Passerat de Silans, I. Maurin, P. Chaves de Souza Segundo, S. Saltiel, M.-P. Gorza, M. Ducloy, D. Bloch, D. de Sousa Meneses, and P. Echegut, *Temperature dependence of the dielectric permittivity of CaF_2 , BaF_2 and Al_2O_3 : Application to the prediction of a temperature-dependent van der Waals surface interaction exerted onto a neighbouring $\text{Cs}(8P_{3/2})$ atom*, *J. Phys.: Condens. Matter* **21**, 255902 (2009).
- [3] H. Haug and S. W. Koch, *Quantum Theory of the Optical and Electronic Properties of Semiconductors* (World Scientific, Singapore, 2009).
- [4] U. D. Jentschura, *Advanced Classical Electrodynamics: Green Functions, Regularizations, Multipole Decompositions* (World Scientific, Singapore, 2017).
- [5] C. Moore, C. M. Adhikari, T. Das, L. Resch, C. A. Ullrich, and U. D. Jentschura, *Temperature-dependent dielectric function of intrinsic silicon: Analytic models and atom-surface potentials*, *Phys. Rev. B* **106**, 045202 (2022).
- [6] C. Moore, C. M. Adhikari, T. Das, L. Resch, C. A. Ullrich, and U. D. Jentschura, *Erratum: Temperature-dependent dielectric function of intrinsic silicon: Analytic models and atom-surface potentials*, submitted.
- [7] M. W. Ribarsky, *Titanium Dioxide (TiO_2) (Rutile)*, in *Vol. II of the Handbook of Optical Constants of Solids*, pp. 795–804, (E. D. Palik, Ed.), Academic Press, Boston, 1985.
- [8] W. J. Tropsf, *Cubic Thallium (I) Halides*, in *Vol. III of the Handbook of Optical Constants of Solids*, pp. 923–967, (E. D. Palik, Ed.), Academic Press, Boston, 1985.
- [9] E. D. Palik and R. Khanna, *Sodium Nitrate (NaNO_3)*, in *Vol. III of the Handbook of Optical Constants of Solids*, pp. 873–881, (E. D. Palik, Ed.), Academic Press, Boston, 1985.
- [10] U. D. Jentschura, *Revisiting the Divergent Multipole Expansion of Atom-Surface Interactions: Hydrogen and Positronium, α -Quartz, and Physisorption*, *Phys. Rev. A* **109**, 012802 (2024).
- [11] U. D. Jentschura and G. S. Adkins, *Quantum Electrodynamics: Atoms, Lasers and Gravity* (World Scientific, Singapore, 2022).
- [12] In principle, the derivations presented here could be generalized to oscillators with different masses m_1 , m_2 , and so on. This would somewhat complicate the derivations but would not alter our conclusions.
- [13] N. W. Ashcroft and N. D. Mermin, *Solid state physics* (Saunders College, Fort Worth, 1976).
- [14] J. H. Hannay, *The Clausius-Mossotti equation: an alternative derivation*, *Eur. J. Phys.* **4**, 141 (1983).
- [15] J. K. Freericks and E. H. Lieb, *Ground state of a general electron-phonon Hamiltonian as a spin singlet*, *Phys. Rev. B* **51**, 2812–2821 (1995).
- [16] J. Flick, D. M. Welakuh, M. Ruggenthaler, H. Appel, and A. Rubio, *Light-Matter Response in Non-Relativistic Quantum Electrodynamics: Quantum Modifications of Maxwell's Equations*, *ACS Photonics* **6**, 2757–2778 (2019).
- [17] P. Hohenberg and W. Kohn, *Inhomogeneous Electron Gas*, *Phys. Rev.* **136**, B864–B871 (1964).
- [18] W. Kohn and L. J. Sham, *Self-Consistent Equations Including Exchange and Correlation Effects*, *Phys. Rev.* **140**, A1133–A1138 (1965).
- [19] C. E. Patrick and F. Giustino, *Unified theory of electron-phonon renormalization and phonon-assisted optical absorption*, *J. Phys.: Condens. Matter* **26**, 365503 (2014).
- [20] F. Giustino, *Electron-phonon interactions from first principles*, *Rev. Mod. Phys.* **89**, 015003 (2017).
- [21] B. Monserrat, C. E. Dreyer, and K. M. Rabe, *Phonon-assisted optical absorption in BaSnO_3 from first principles*, *Phys. Rev. B* **97**, 104310 (2018).
- [22] T. Das, C. A. Ullrich, and U. D. Jentschura, *Temperature-Dependent Dielectric Function of Calcium Difluoride (CaF_2): Infrared and Ultraviolet Contributions*, in preparation (2025).
- [23] H. H. Li, *Refractive Index of Alkaline Earth Halides and Its Wavelength and Temperature Derivatives*, *J. Phys. Chem. Ref. Data* **9**, 161–290 (1980).
- [24] D. F. Bezuidenhout, *Calcium Fluoride (CaF_2)*, in *Handbook of Optical Constants of Solids, Vol. 2*, pp. 815–828, (E. D. Palik, Ed.), Academic Press, Boston, 1985.
- [25] M. Daimon and A. Masumura, *High-Accuracy Measurements of the Refractive Index and Its Temperature Coefficient of Calcium Fluoride in a Wide Wavelength Range from 138 to 2326 Nm*, *Appl. Opt.* **41**, 5275 (2002).
- [26] D. B. Leviton, K. H. Miller, M. A. Quijada, and F. U. Grupp, in *SPIE Optical Engineering + Applications, Proceedings Volume 9578*, edited by R. B. Johnson, V. N. Mahajan, and S. Thibault (SPIE Press, San Diego, California, United States, 2015), pp. 1–12.
- [27] M. R. K. Kelly-Gorham, B. M. DeVetter, C. S. Brauer, B. D. Cannon, S. D. Burton, M. Bliss, T. J. Johnson, and T. L. Myers, *Complex Refractive Index Measurements for BaF_2 and CaF_2 via Single-Angle Infrared Reflectance Spectroscopy*, *Opt. Mat.* **72**, 743–748 (2017).
- [28] Q. Zheng, X. Wang, and D. Thompson, *Temperature-Dependent Optical Properties of Monocrystalline CaF_2 , BaF_2 , and MgF_2* , *Opt. Mater. Express* **13**, 2380 (2023).